A. Gritsenko
Doctor
South Ural State University
Automobile and Tractor Faculty
Russia

V. Shepelev
Ph.D
South Ural State University
Automobile and Tractor Faculty
Russia

A. Burzev
Ph.D
Kuzbass State Technical University
named after T.F. Gorbachev
Department of Mining and
Technosphere Safety
Russia

G. Salimonenko
Ph.D.student
South Ural State University
Automobile and Tractor Faculty
Russia

A Study of the Output Characteristics of Electric Fuel Pumps during Artificial Fault Simulation

The electric fuel pump (EFP) is one of the potential sources of fuel system failures. According to various data, the fuel system accounts for 25...50% of all failures. The most common reason for the impairment of the fuel system performance and, in particular, the failure of the fuel pump is the contamination of fuel with large or small particles, as well as the wear of the structural elements of the EFP. The purpose of the study is to determine the technical condition of electric fuel pumps of motor vehicle engines based on the use of testing technologies. The paper discusses theoretical and experimental studies of the fuel system of motor vehicle engines: the change in the current consumption rate of the EFP depending on the degree of contamination of series elements in the system and leaks in the injection unit of the EFP.

Keywords: *fuel supply system, fuel pump, diagnostics, clogging, leaks, current rate, voltage, fuel supply line section.*

1. INTRODUCTION

The weakest component in the EFP is the injection unit, whose service life is not determined in the operating conditions of motor vehicle engines [1]. The service life may be determined through the use of testing methods [2, 3, 4]. Technological failures of the EFP are divided into two types: mechanical and electrical [5, 6]. The main signs of the impairment of the fuel pump performance are unstable engine operation, interrupted fuel supply, increased leaks in the injection unit of the EFP, slow acceleration of the vehicle due to a violated fuel supply, delayed acceleration of the ICE when the accelerator pedal is activated, uneven fuel supply on the move, as well as related pump failures - increased noise during the pump operation, pops in the dumper [7, 8]. All this jointly worsens the performance of the ICE up to its shutdown [9, 10, 11].

The research hypothesis - an increase or decrease in the current rate due to clogging (increased resistance of fuel supply elements) or as a result of the wear of the injection unit (increased leaks) - can be taken as a testing parameter of its technical condition in the course of testing the EFP.

The following tasks should be solved to achieve the set objective:

1. To establish the relationship between the rate of the fuel supply and its pressure when the technical condition of the power-supply line worsens (increased clogging or leaks) with the current rate in the course testing the EFP;

2. To justify the technology of the testing method and the testing parameter for assessing the technical condition of the EFP;

3. To develop a methodology, to carry out experimental research.

Notably, one of the reasons for the high content of mechanical impurities in the fuel tanks is the high dust content of the atmospheric air in the area of operation [12]. The composition is dominated by dust consisting of 60–70% of mineral particles (silica, oxides of aluminium, calcium, and magnesium), as well as of organic substances. Over 70% of the dust fraction composition is up to 1 μm.

Unfortunately, the problem of ensuring the necessary purity of the fuel supplied to the precision units of the fuel pumps in mobile vehicles remains unsolved today due to the low efficiency of preliminary and primary purification of fuel in the fuel system [13, 14]. This is evidenced by the fact that even in fresh oil products, as well as in the tanks of new vehicles, which have not yet accumulated impurities, the content of small particles of up to 5 μm is about 30%.

Alongside with that, the consequences of changing the technical condition of the fuel system should be corrected using a microprocessor control system (MPCS), which can be explained in Fig 1.

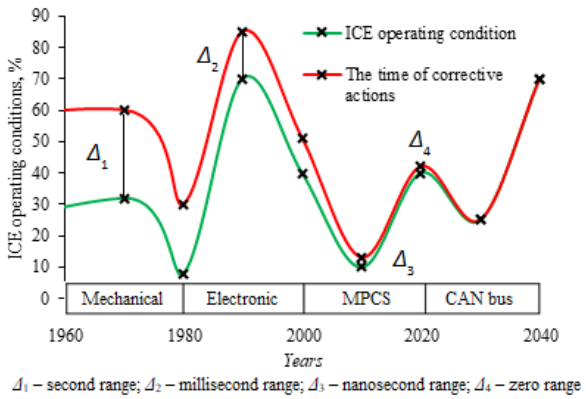

Figure 1. The dependence of the time of corrective actions on the ICE operating conditions

Received: January 2020, Accepted: March 2021
Correspondence to: Ph.D Vladimir Shepelev
South Ural State University, Automobile and Tractor Faculty , Lenin Avenue 76, 454080 Chelyabinsk, Russia
E-mail: shepelevvd@susu.ru
doi:10.5937/fme2102480G

Let us analyse Fig. 1. So, in 1960-1980 the response to performance changes in the ICE parameters was carried out through the use of mechanical control, the response duration Δ_1 was in the second range. In 1980-2000 ICE systems were controlled through the use of the first electronic units (FEU), the response duration Δ_2 was in the millisecond range. Currently, in 2000-2020 ICE systems are controlled through the use of the microprocessor system (MPCS), the response duration Δ_3 corresponds to the nanosecond range. In the long term of 2020-2040 the signal will be transmitted to any ICE component through the use of the CAN bus, where the response range Δ_4 will be picoseconds.

Consequently, a higher EFP performance is needed, since its effect influences the correctness of the ICE operation.

2. THEORETICAL RESEARCH

The purpose of this theoretical research is to establish the relationships and regularities of the fuel supply process used as a basis for the justification of the testing parameter and the development of the testing technology, allowing us to assess the level of the EFP performance [15].

The novelty of the approach lies in the recognition of the technical condition of the electric fuel pumps of modern vehicles by means of an integrated control of the mechanical, electrical, and hydraulic parts of the EFP. To this end:

1. A test mode is created in the form of a change in the supply voltage of the EFP, and a response to the test action is tracked in the form of a degree of decrease in the pressure and supply of the EFP in simulated critical conditions.
2. When simulating artificial clogging of the fuel supply line by installing a series resistance (jet), the limiting values of the decrease in supply and pressure are justified in case of a failure condition of the EFP. Besides, the limiting values of the current load (current rate values) are set for detecting the limiting values of the clogging degree of the fuel filters and fuel lines.
3. When installing hydraulic resistances (jets) in the fuel supply line parallel to the EFP, the limiting decreases in the pump supply current connected with a decrease in hydraulic resistance in the common fuel supply line are determined. On this basis, faults are divided into increased and decreased hydraulic resistance of the fuel supply line.
4. When simulating the limiting conditions by installing jets and reducing the supply voltage, there appear favorable conditions for observing the EFP wedging and recognizing hidden defects and accumulating defects, which cause the EFP wedging.
5. A complex algorithm for determining the technical condition of the fuel supply system and EFP, in particular, during sequential test inputs, is formed.

In this research, we focused on the experimental study of the parameters of the current rate, voltage, and resistance of the EFP, depending on the change in the size of the flow passage of the filter element. The obtained theoretical dependences of the change in the current consumption rate on the parameters of the fuel supply, pressure, and rotor speed can be taken as diagnostic indicators when determining the technical condition of the EFP.

When studying the serial fuel supply process, it is necessary to develop a mathematical model for describing the formation of the fuel pressure, supply, total energy consumption of the EFP, and the value of the electrical parameters I, U, R.

The electric pump is a compulsory structural and technical element of the fuel system with the parameters determining the value of the functional (P, Q, n), electrical (I, U, R), and structural parameters (ε, y). Therefore, when the functional parameters change by Δ (ΔP, ΔQ) during operation, they are related with the electrical parameters I, U, R. Our research and analytical description will allow us to justify the testing parameter of the technical condition of the EFP.

Let us analyse the balance of the supplied and transferred energies in the power system. To this end, we will consider the dependence of the supplied energy on the current source to the supply line (E_{pot}) with the energy for the movement of the liquid in the fuel line (E_{pered}):

Let us analyse the balance of the delivered and transmitted energy in the supply system [16, 17, 18]. To this end, let us consider a dependence of the energy delivered from the current source to the EFP (E_{del}) with the liquid movement energy in the fuel supply line (E_{trans},):

$$E_{del} = E_{trans} . \tag{1}$$

where E_{del} is the energy delivered to the EFP, J; E_{trans} is the energy transmitted by the pump during the fuel supply, J.

Let us consider the left side of the EFP energy balance equation. The delivered energy E_{del} is determined by the expression:

$$E_{del} = I \cdot U \cdot t . \tag{2}$$

where I is the current consumption rate of the EFP, A; U is the supply voltage at the EFP terminals, V; t is the pump run time, s.

Let us consider the consumable of the energy balance. The transmitted energy E_{trans} diverges to the following components:

$$E_{trans} = E_{el.loss} + E_{hyd.loss} + A_{yield} . \tag{3}$$

where $E_{el.loss}$ is energy loss in the electrical circuits of the pump, J; $E_{hyd.loss}$ is energy consumption for hydraulic losses, J; A_{yield} is the useful yield of the EFP to supply the fuel, J.

Substituting special formulas into Eq. (3) and making transformations with regard to the current consumption rate I, we obtain:

$$I = U\left(\frac{1}{R} + \frac{\Delta P - \Delta P_{reg}}{\rho \cdot g} + \mu \cdot S_{tot}\sqrt{\frac{2\left(\Delta P - \Delta P_{reg}\right)^2}{\rho}}\right). \tag{4}$$

where the right side of the Eq. (4) represents the generalized resistance of the fuel system; ΔP are pressure drops at the sections, Pa; ΔP_{reg} is the pressure drop on the fuel rail regulator, Pa; ρ is the fuel density, kg/m^3; g is the acceleration of gravity, m/s^2; μ is the flow coefficient; S_{tot} is the total area of the clearances in the filter section, or the total area of the clearances between the pump rollers and housing, m^2.

In case of a series connection of hydraulic resistances, S_{tot} is determined by the Eq. (5):

$$\mu \cdot S_{tot} = \mu \cdot S_1 + \mu \cdot S_2 . \quad (5)$$

where S_1 is the passage area in the filter section, m^2; S^2 is the area of the clearances between the EFP rollers and housing, m^2.

In case of a parallel connection of hydraulic resistances, S_{tot} is determined by the Eq. (6):

$$\frac{1}{\mu \cdot S_{tot}} = \frac{1}{\mu \cdot S_1} + \frac{1}{\mu \cdot S_2} . \quad (6)$$

Thus, we established the dependence of the current rate of the EFP I on the electrical parameters of the drive motor (U, R) with the structural and functional parameters of the EFP ($\mu \cdot S$, ΔP, Q).

Let us model the regularities of changes in the current consumption rate of the EFP in the fuel system I depending on the supply voltage U (according to Eq. (4)) for various technical conditions of the fuel supply system elements $\mu \cdot S_{tot}$. The studied ZMZ-406.2 engine is equipped with an *In-Line* fuel pump with a nominal capacity of Q=130 *l/h* = 0.0000361 m^3/s, the current consumption I=3.1 A, n=2800 min^{-1}. The pressure regulator in the fuel rail is set to a maximum pressure of P=310 kPa=310,000 Pa=310,000 N/m^2. The excess fuel unused during the fuel injection is discharged via the fuel return line to the fuel tank. The EFP is designed to operate at a nominal voltage of U_{const}=12 V. If the EFP corresponds to the technical reference condition, the electrical loss is minimal, and is N_{el}=5 B=*const*. Let us build the dependencies of I on U at three points: at U_1=6.5 V; U_2=9.5 V; U_3=12.5 V, and, respectively, the diameters of the flow passage of 0.2 mm, 1.2 mm and 7 mm (reference).

Fig. 2 shows the results of calculations by the Eq. (4).

It can be seen from the analysis of Fig. 2 that when the diameter of the flow passage decreases to 0.2 mm (i.e., the hydraulic resistance increases), for example, a fine fuel filter becomes clogged, the current consumption rate increases significantly from 2.3 A to 5.2 A The increase in the current rate is connected with an increase in the hydraulic resistance in the fuel system □. An increase in the hydraulic resistance leads to a rise in the EFP rotor counter-torque. As a result, the rotor spins under load, and increased current is consumed I.

Fig. 3 shows that with an increase in the diameter of leaks, l (worn rollers of the injection unit of the EFP), the current rate decreases.

An increase in the amount of the clearances between the EFP rollers and housing leads to an increase in fuel leakage. The fuel is pumped back into the pressure cavity of the pump. As a result, the fuel is not pumped into the fuel supply line, or a small part of it is pumped, and its bulk returns to the suction cavity (recirculation).

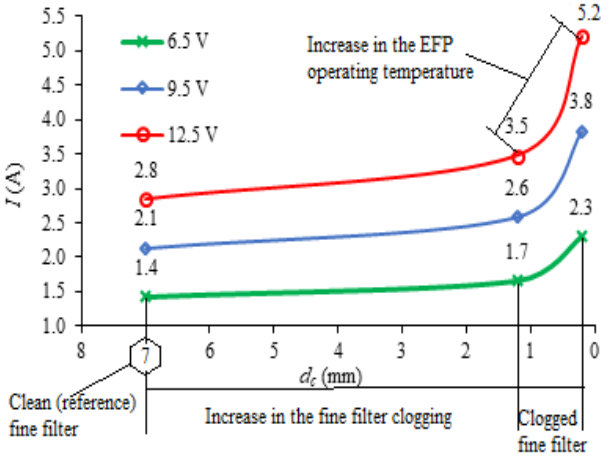

7 mm=38.465 mm^2 is the reference section when the fuel filter is clean; 1.2 mm=1.1304 mm^2 is the diameter of the flow passage less than the reference one (increased clogging); 0.2 mm=0.0314 mm^2 is a very small flow passage equal to the extremely clogged fine filter

Figure 2. Regularities of changes in the current rate *I* depending on the diameter of the fuel supply line section d_s (modelling of the filter element clogging *I=f(□)*)

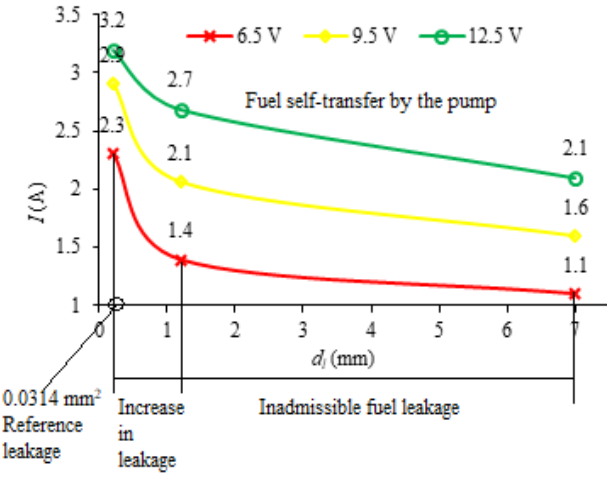

0.2 mm=0.0314 mm^2 is the reference amount of the clearances between the EFP rollers and housing; 1.2 mm=1.1304 mm^2 is the increase in the amount of the clearances between the EFP rollers and housing; 7 mm=38.465 mm^2 is the maximum amount of the clearances.

Figure 3. Regularities of changes in the current rate *I* depending on the diameter of a fuel leak in the fuel system d_l (modelling of leakage in the EFP housing *I=f(y)*)

Fig. 4 shows a dependence of the change in the current consumption rate of the EFP at simultaneously increasing leaks in the EFP l and the resistance in the fuel system ε in a three-dimensional coordinate system.

An analysis of Fig. 4 shows that the supply current rate of the EFP decreases with an increase in leakage and vice versa increases with an increase in clogging. Thus, the current is a sensitive parameter, which increases or decreases depending on the increase or decrease in clogging and leaks in the fuel system and the EFP, which suggests that it can be taken as a testing parameter.

3. RESEARCH METHODOLOGY. PLANNING OF A THREE-FACTOR EXPERIMENT

The purpose of the multi-factor experiment was to determine the degree of impact of the calibrated orifices of jets installed simultaneously in the fuel system at series and parallel connection, as well as the effect of the EFP supply voltage set by the control unit on the current consumption rate of the EFP I, the pressure in the supply system P and the amount of fuel leakage Q. The experiment was carried out according to the scheme in Fig. 5.

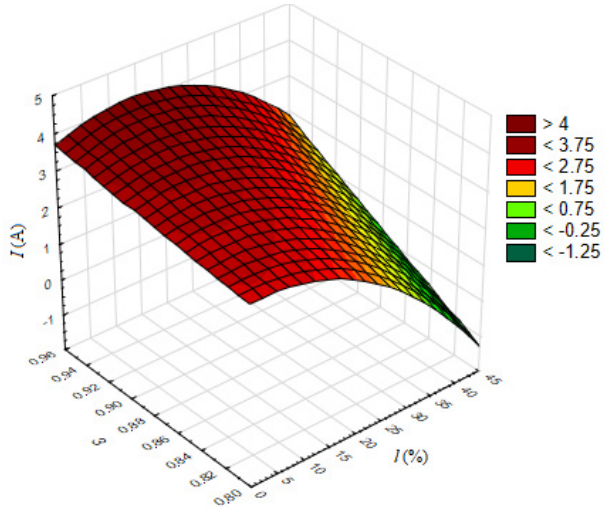

Figure 4. The dependence of the change in the current consumption rate of the EFP *I* at simultaneously changing leaks *I* and clogging (resistance □ *(axis 2)*)

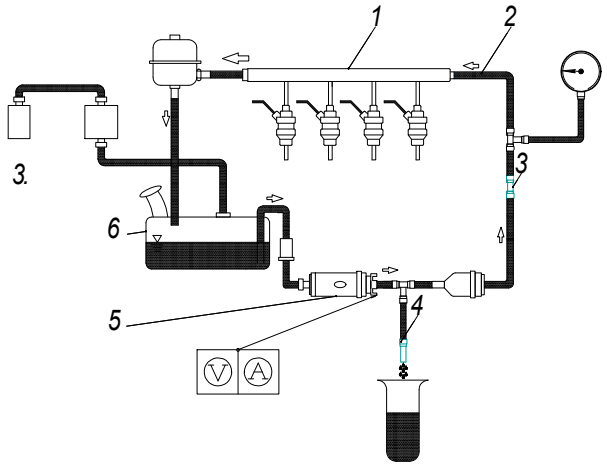

1 – fuel rail; 2 – fuel supply line; 3 – series jet; 4 – parallel jet; 5 – fuel pump; 6 – fuel tank

Figure 5. Scheme of the three-factor experiment

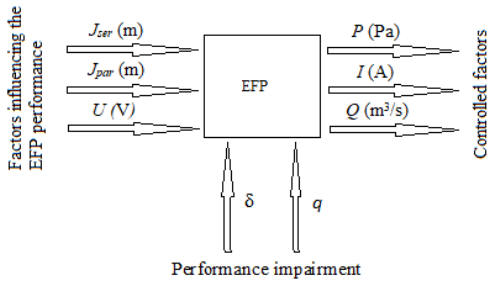

Figure 6. Input and output parameters during the three-factor experiment

For parallel connection, we installed calibrated jets J_{par} of 0.2 mm, 0.6 mm, 1.0 mm, with the variation interval Δ=0.4 mm. For series connection, we installed J_{ser} of 0.2 mm, 0.7 mm, 1.2 mm in the fuel supply line, with an interval Δ=0.5 mm. This experiment was also carried out with an artificial simultaneous simulation of fuel leaks in the EFP housing and clogging of the fuel filters. The control unit set 3 voltage values of 6.5 V, 9.5 V, and 12.5 V.

The controlling factors are J_{ser} – the diameter of the calibrated orifice of the jet connected in series to the fuel supply line, m; J_{par} – the diameter of the calibrated orifice of the jet connected in parallel to the fuel supply line, m; U – the supply voltage of the EFP set by the Vympel-50 external control unit, V.

The steady state values (response) are the following indicators: the power consumption rate of the EFP, I, the pressure in the supply system P, and the amount of fuel leakage Q. The intervals and levels of factor variations are given in Table 1.

Table 1. Levels and intervals of factor variations

Factor	Desig-nator	Variation level			Interval, Δ
		-1 (lower)	0	+1 (upper)	
Series calibrated jet, J_{ser}, m.	$M_{i,1}$	0.3	0.75	1.2	0.45
Parallel calibrated jet, J_{par}, m.	$M_{i,2}$	0.2	0.6	1	0.4
Supply voltage of the EFP, U, V.	$M_{i,3}$	6.5	9.5	12.5	3

Based on the assumption that in this case three factors influencing the optimization parameters (vy_1, vy_2, vy_3) are considered, we should carry out a three-factor experiment, which is described by the general regression equation:

$$vy_i^{1,2,3} = a_1 \cdot \left(M_{i,1}\right)^{a2} + b_1 \cdot \left(M_{i,2}\right)^{b2} + \\ + c_1 \cdot \left(M_{i,3}\right)^{c2} + g \cdot M_{i,1} \cdot M_{i,2} + \\ + m \cdot M_{i,1} \cdot M_{i,3} + nM_{i,2} \cdot M_{i,3} \quad (7)$$

where $M_{i,1}$, $M_{i,2}$, $M_{i,3}$ are the values of the controlled factors; a_1, b_1, c_1 are regression coefficients of the relevant factors indicating the effect of one or another factor on the studied process; g, m, n are regression coefficients in the product of the factors indicating the presence of a double effect between the factors; a_2, b_2, c_2 are regression coefficients indicating the presence of an interaction between the factors; vy_1, vy_2, vy_3 are the output parameters, respectively (I, Q, P).

We find the variation interval ΔM_i for each factor value:

$$\Delta M_i = \frac{M_i^U - M_i^L}{2} \quad (8)$$

where M_i^U, M_i^L are the values of the factors at the upper and lower levels, respectively; ΔM_i is the natural value of the factor variation interval; i is the factor number.

These level values are determined for each factor.

The encoded value of the factor M_i is determined by the Eq. (9):

$$M = \frac{M_i - M_{main}}{\Delta M_i}. \quad (9)$$

where M is the natural value of the factor; M_{main} is the factor value at the main level.

Let us determine the number of points N of the plan of the three options:

$$N = 3^k. \quad (10)$$

where 3 is the number of levels; k is the total number of factors, 3.

In this case, N=27.

The regression coefficients are calculated in the Mathcad 14 software by the Minerr function. Let us present them in Table 2.

Table 2. Regression coefficients

Coefficients	(*I*)	(*Q*)	(*P*)
1	2	3	4
a_1	0.978	-1.27	12.328
a_2	0.495	1.856	1.1
b_1	0.052	294.986	33.133
b_2	-2.026	2.338	-0.568
c_1	2.049	0.939	-0.025
c_2	2.154	-3.261	-2.921
g	0.263	56.125	2.808
m	-0.4	9.715	2.82
n	-0.667	-472.949	33.585

The regression equations, taking into account their obtained coefficients, will take the following form:

For the pressure:

$$P(M_{i3};M_{i2};M_{i1}) = 12.328 \cdot M_{i3}^{1.1} + \\ +33.133 \cdot M_{i2}^{-0.568} - 0.025 \cdot M_{i1}^{-2.921} + \\ +2.808 \cdot M_{i3} \cdot M_{i2} + 2.82 \cdot M_{i3} \cdot M_{i1} + \\ +33.585 \cdot M_{i2} \cdot M_{i1} \quad (11)$$

For leakage:

$$Q(M_{i3};M_{i2};M_{i1}) = -1.27 \cdot M_{i3}^{1.856} + \\ +294.986 \cdot M_{i2}^{2.338} + 0.939 \cdot M_{i1}^{-3.261} + \\ +56.125 \cdot M_{i3} \cdot M_{i2} + 9.715 \cdot M_{i3} \cdot M_{i1} - \\ -472.949 \cdot M_{i2} \cdot M_{i1} \quad (12)$$

For the current rate:

$$I(M_{i3};M_{i2};M_{i1}) = 0.978 \cdot M_{i3}^{0.495} + \\ +0.052 \cdot M_{i2}^{-2.026} + 2.049 \cdot M_{i1}^{2.154} + \\ +0.263 \cdot M_{i3} \cdot M_{i2} - 0.4 \cdot M_{i3} \cdot M_{i1} - \\ -0.667 \cdot M_{i2} \cdot M_{i1} \quad (13)$$

Using such equations, the researcher eliminates the need to transfer the experimental conditions each time into encoded variables.

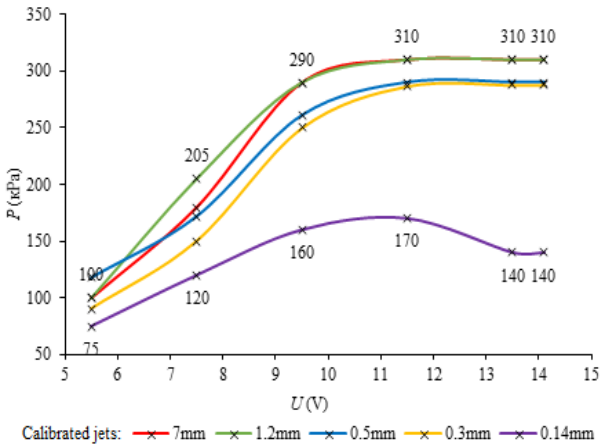

Figure 7. The dependence of the pressure change in the supply system on the voltage of the EFP when using calibrated jets of various flow passage diameters (0.14 mm...7 mm)

4. THE RESULTS OF THE EXPERIMENTAL STUDIES USING THE CALIBRATED JETS CONNECTED IN SERIES TO THE FUEL SUPPLY LINE

During the experimental studies with a series connection of the calibrated jets, we obtained the data in the form of a graphical dependence of the change in the current rate on the supply voltage of the EFP (Fig. 7), and the pressure on the supply voltage of the EFP (Fig. 8).

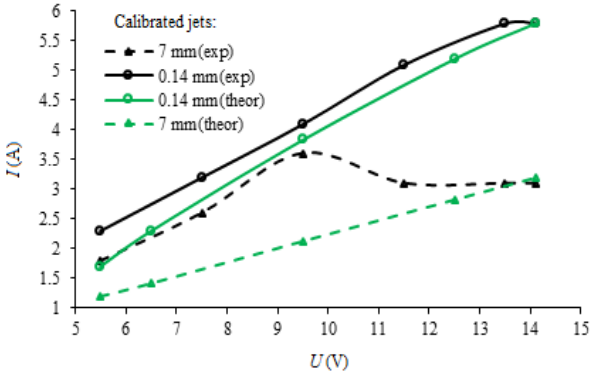

Figure 8. The dependence of the change in the current consumption rate of the EFP on the voltage supplied to the pump by the external control unit when using calibrated jets with the following section diameters (0.14 mm…7 mm)

When the EFP is operated without calibrated jets, a steady state pressure of 310 kPa is observed at a voltage of 10 V (Fig. 7), and the current rate reaches 3.1 A (Fig. 8). In this case, the EFP freely pumps the fuel into the line without much effort, i.e., the resistance after the pump is equal to the standard one, and there is no artificial resistance.

When the EFP operates with a minimum calibrated jet equal to 0.14 mm, reduced pressure is observed throughout the entire range of the supply voltage increase, which is necessary for the proper operation of the ICE, while the supply current increases all the time.

The increase in the supply current (5...6 A) is explained by the fact that the injection unit of the EFP

pushes the required amount of fuel forcedly through a minimum orifice equal to 0.14 mm. As a result, we obtained the data on the steady state current rate and pressure of the EFP at the maximum value of the artificially simulated resistance in the fuel line, which is equal to the clogged state of the fuel filter screen and the fuel wire (Table 3).

Table 3. Comparison of the calculated and experimental indicators

Voltage U, V	Current consumption rate I, A				Error, %	
	$0{,}14^{C}$ mm	$0{,}14^{E}$ mm	7^{C} mm	7^{E} mm	0.14 mm	7 mm
5.5	1.7	2.3	1.8	1.2	17.6	25
6.5	2.3	2.7	2.2	1.42	8.65	22.5
9.5	3.83	4.1	3.6	2.13	3.5	35
12.5	5.2	5.6	3.1	2.83	3.85	4.75
14.1	5.8	5.8	3.1	3.2	0	1.6
Average error, %					6.72	13.27

When the EFP operates with other jets of 1.2 mm, 0.5 mm, 0.3 mm, a steady state pressure of 310 kPa is observed, but the supply current corresponds to a value exceeding the nominal of 3.1 A. In this case, when clogging increases, the injection unit of the EFP overcomes the resistance to the fuel movement in the system.

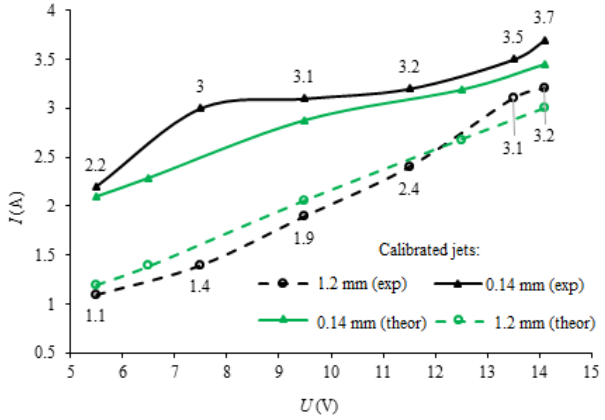

Figure 9. The dependence of the change in the current consumption rate of the EFP on the change in the supply voltage when using calibrated flow passage jets (0.14 mm...1.2 mm) connected in parallel to the fuel supply line

5. THE RESULTS OF THE EXPERIMENTAL STUDIES USING THE CALIBRATED JETS CONNECTED IN PARALLEL TO THE FUEL-SUPPLY LINE

During the experimental studies when the jets we connected in parallel, we obtained the data presented in the form of the dependencies of the change in the current rate on the supply voltage of the EFP (Fig. 9), as well as the change in the pressure on the supply voltage of the EFP (Fig. 10).

When the EFP operates with a jet equal to 1.2 mm, reduced pressure is observed throughout the entire range of the change in the supply voltage of the EFP (Fig. 10). The maximum values of the pressure and current rate at a voltage of 14.1 V were 275 kPa and 3.1 A, respectively (Fig. 9). Such values are explained by the fact that the bulk of the fuel is lost through a parallel jet with a cross-section of 1.2 mm, and only a small amount of the fuel enters the line.

The maximum and minimum errors in the experiment when using a calibrated jet of 0.14 mm are 8.95% and 2.35%, respectively, and when using a jet of 1.2 mm - 4.2% and 1.5% (Table 4).

Table 4. Comparison of the calculated and experimental indicators

Voltage U, V	Current consumption rate I, A				Error, %	
	$0{,}14^{C}$ mm	$0{,}14^{E}$ mm	$1{,}2^{C}$ mm	$1{,}2^{E}$ mm	0,14 mm	1,2 mm
5.5	2.1	2.2	1.2	1.1	2.35	4.5
6.5	2.29	2.7	1.39	1.3	8.95	3.45
9.5	2.88	3.1	2.06	1.9	3.8	4.2
12.5	3.19	3.3	2.68	2.6	1.7	1.5
14.1	3.45	3.7	3	3.2	3.6	3.3
Average error, %					4.08	3.39

When the EFP operates with a drain jet of 0.14 mm, a steady state pressure of 310 kPa is observed at a voltage of 9.5 V. At the same time, the nominal current rate is set to 3.1 A. In this case, the injection unit freely supplies the fuel to the main line without much effort, losses through this calibrated jet are negligible, and therefore the bulk of the fuel is supplied further into the fuel supply line after the jet.

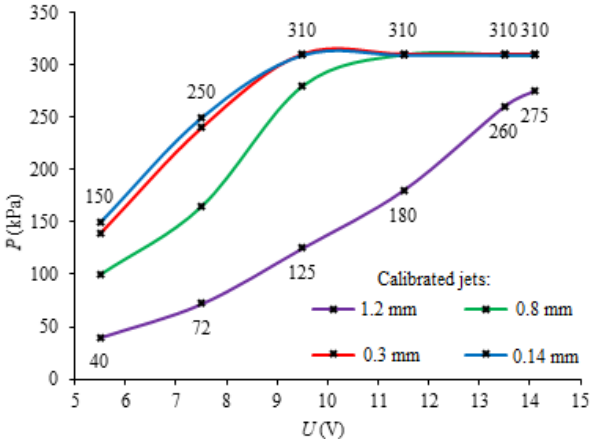

Figure 10. The dependence of the change in the pressure in the supply system on the voltage supplied to the EFP when using calibrated flow passage jets (0.14 mm...1.2 mm) connected in parallel to the fuel supply line

When the EFP operates with the remaining jets of 0.8 mm, 0.3 mm, a steady state pressure of 310 kPa, and a current consumption rate of 3.1 A are observed. In this case, fuel leaks are equal to the average value through the parallel calibrated jet. Despite this the EFP is able to pump the required fuel amount into the main line.

6. CONCLUSION

The results of the experiment showed that when the EFP operates with a minimum calibrated jet of 0.14 mm installed in series in the section of the fuel supply line, an unsteady state pressure is observed throughout the entire range of the voltage increase from 5.5 to 14.1 V. In this case, the supply current reached the values from 5 to 6 A because the injection unit of the EFP forces the fuel through a small orifice of 0.14 mm.

The results of the experiment showed that when the EFP operates with a calibrated jet of 1.2 mm installed in parallel to the fuel system to drain, an unstable state reduced pressure is observed throughout the entire range of the supply voltage increase of the EFP. The maximum steady state values of the pressure and current rate at a voltage of 12.5 V are 220 kPa and 2.7 A, respectively. Such values are explained by the fact that the bulk of the fuel is lost through the jet connected in parallel to the fuel supply line.

REFERENCES

[1] Erokhov, V. I.: *Injection systems of gasoline engines (design, calculation, diagnostics)*, Hot line - Telecom, Moscow, 2011.

[2] Hsu, P., Lin, K. and Shen, L.: Diagnosis of multiple sensor and actuator failures in automotive engines, IEEE Transactions on Vehicular Technology, Vol. 44, No. 4, pp. 779-789, 1995.

[3] Salikhov, R.F., Makushev, Y.P., Musagitova, G.N., Volkova, L.U. and Suleymanov, R.S.: Diagnosis of fuel equipment of diesel engines in oil-and-gas machinery and facilities, in: *Proceedings of the AIP Conference Proceedings on Oil and Gas Engineering Conference,* 26-28.02.2019, Omsk, Russian Federation, Paper 2141.

[4] Miljić, N. L.and Popović, S. J.: Model based tuning of a variable-speed governor for a distributor fuel-injection pump, FME Transactions, Vol. 42, No. 1, pp. 40-48, 2014.

[5] Vlasov, D.B. et al.: Methodological aspects of diagnostics of electric gasoline pumps in operation of automobiles, Lecture Notes in Mechanical Engineering, No. 9783319956299, pp. 2193-2201, 2019.

[6] Wang, Z., Qian, Y., Wang, L., Zhang, S. and Luo, X.: The extraction of hidden fault diagnostic knowledge in equipment technology manual based on semantic annotation, in: *Conference Proceeding Series of 8th International Conference on Software and Computer Applications*, 19-21.02.2019, Usains Holding Sdn BhdPenang, Malaysia, Part F147956, pp. 419-424.

[7] Yakimov, I. V., Krivtsov, S. N., Potapov, A. S. and Svirbutovich, O. A.: Fuel flow and pressure in common return line as a diagnostic parameter of electro-hydraulic injectors technical state, in: *Proceedings of IOP Conference Series: Materials Science and Engineering on 2019 International Conference on Innovations in Automotive and Aerospace Engineering*, 27.05-01.06. 2019, Irkutsk, Russian Federation, Vol. 632, No.1.

[8] Krogerus, T. R., Hyvönen, M. P. and Huhtala, K. J.: A survey of analysis, modelling, and diagnostics of diesel fuel injection systems, Journal of Engineering for Gas Turbines and Power, Vol. 138, No.8, 2016.

[9] Kurnykina, O.V., Popova, O.V., Zubkova, S.V., Karpukhin, D.V., Pavlov, V.P., Varenik, P.K., Aleshkova, I.A. and Novitskaya, L.Y.: Air pollution by road traffic and its measurement methods, EurAsian Journal of BioSciences, Vol. 12, No. 2, pp. 181-188, 2018.

[10] Tormos, B., Martín, J., Carreño, R. and Ramírez, L.: A general model to evaluate mechanical losses and auxiliary energy consumption in reciprocating internal combustion engines, Tribology International, No. 123, pp. 161-179, 2018.

[11] Jiao, X., Jing, B., Qiang, X., Liu, X., Li, J. and Zhou, W.: Fault diagnosis and test platform for airborne fuel pumps, Zhendong Yu Chongji/Journal of Vibration and Shock, Vol. 36, No.1, pp. 120-128, 2017.

[12] Chen, S., Liu, W., Tsai, J. and Hung, I.: Vehicle fuel pump service life evaluation using on-board diagnostic (OBD) data, in: *Proceedings of the 2016 International Conference on Orange Technologies*, 18-20.12.2018, Melbourne, Australia, pp.35-84.

[13] Jiao, X., Jing, B., Huang, Y., Liang, W. and Xu, G.: A fault diagnosis approach for airborne fuel pump based on EMD and probabilistic neural networks, in: *Proceedings of 2016 Prognostics and System Health Management Conference on 7th IEEE Prognostics and System Health Management Conference*, 19-21.10.2017, Sichuan, China.

[14] Liu, X., Jing, B., Shi, H., Qiang, X. and Sheng, Z.: Optimized design of fuel pump fault diagnosis experimental device and test program, Zhendong Ceshi Yu Zhenduan/Journal of Vibration, Measurement and Diagnosis, Vol. 37, No. 6, pp. 1187-1194 and 1281, 2017.

[15] Gritsenko, A., Kukov, S. and Glemba, K.: Theoretical underpinning of diagnosing the cylinder group during motoring, in: *Proceedings of 2nd International Conference on Industrial Engineering,* 19-20.05.2016, Chelyabinsk, Russian Federation, No. 150, pp. 1182-1187.

[16] Baur, R., Blath, J. P., Bohn, C., Kallage, F. and Schultalbers M.: Modeling and identification of a gasoline common rail injection system, SAE Technical Papers, No. 1, 2014.

[17] Hu, Q., Wu, S. F., Lai, M., Stottler, S. and Raghupathi, R.: Prediction of pressure fluctuations inside an automotive fuel rail system, SAE Technical Papers, 1999.

[18] Ahsan, M.: Prediction of gasoline yield in a fluid catalytic cracking (FCC) riser using k-epsilon turbulence and 4-lump kinetic models: A computational fluid dynamics (CFD) approach, Journal of King Saud University - Engineering Sciences, Vol. 27, No. 2, pp. 130-136, 2015.

ИСТРАЖИВАЊЕ ИЗЛАЗНИХ КАРАКТЕРИСТИКА ЕЛЕКТРИЧНИХ ПУМПИ ЗА ГОРИВО ТОКОМ СИМУЛАЦИЈЕ НАМЕРНО ИЗАЗВАНОГ КВАРА

А. Гритсенко, В. Шепелев, А. Бурзев, Г. Салимоненко

Електрична пумпа за гориво је један од потенцијалних извора квара система за гориво. Према различитим подацима 25 ...50% свих кварова отпада на систем за горива. Перформансе система за гориво, а нарочито квар пумпе за довод горива, угрожава контаминација горива ситним и крупним честицама као и хабање структурних елемената пумпе. Циљ истраживања је да се одреди техничко стање електричне пумпе за гориво код мотора друмског возила применом више технологија испитивања. Разматрају се теоријска и експериментална истраживања система за гориво код мотора друмског возила: промена брзине тренутне потрошње горива у зависности од степена контаминације серијских елемената система и цурење код бризгаљке за гориво код електричне пумпе за гориво.